



## Self-powered elementary hybrid magnetoelectric sensor

Martha Gerhardt<sup>a,1</sup>, Lukas Zimoch<sup>a,1</sup>, Christian Dorn<sup>b</sup>, Eric Elzenheimer<sup>c,d</sup>, Christin Bald<sup>d</sup>, Tjorben Lerg<sup>d</sup>, Johannes Hoffmann<sup>d</sup>, Sören Kaps<sup>a</sup>, Michael Höft<sup>c</sup>, Gerhard Schmidt<sup>d</sup>, Stephan Wulfinhoff<sup>b</sup>, Rainer Adelung<sup>a,\*</sup>

<sup>a</sup> Functional Nanomaterials, Institute for Materials Science, Kiel University, Kaiserstr. 2, 24143 Kiel, Germany

<sup>b</sup> Computational Materials Science, Institute for Materials Science, Kiel University, Kaiserstr. 2, 24143 Kiel, Germany

<sup>c</sup> Chair of Microwave Engineering, Department of Electrical and Information Engineering, Kiel University, Kaiserstr. 2, 24143 Kiel, Germany

<sup>d</sup> Digital Signal Processing and System Theory, Department of Electrical and Information Engineering, Kiel University, Kaiserstr. 2, 24143 Kiel, Germany

### ARTICLE INFO

#### Keywords:

Self-powered  
Energy harvester  
Magnetoelectric Field sensor  
Sensor evaluation  
Sensor modeling

### ABSTRACT

There are numerous magnetic field sensors available, but no simple, robust, sensitive sensor for biomedical applications that does not require cryogenic cooling or shielding has yet been developed. In this contribution, a new approach for building a magnetoelectric field sensor is presented, which has the potential to fill this gap. The sensor is based on a resonant cantilever with a piezoelectric readout layer and a pair of opposing permanent magnets. One is attached to the cantilever, and the other one is fixed to a sample holder below. This new concept can be deduced from the most basic composite-based sensor [1], where the magnets interact analog to two particles in a polymer matrix. The bias-free, empirical measurements show a limit-of-detection of 46 pT/ $\sqrt{\text{Hz}}$  with a sensitivity of 2170 V/T using the sensor's resonance frequency of 223.5 Hz under ambient conditions. The sensor fabrication is based on low resolution silicon technology, which promises high compatibility and the possibility to be integrated into MEMS devices. The design of this new sensor can be easily altered and adjusted according to the requirements of the specific sensor application. For example, tuning of the operating resonance frequency cannot solely be modified in the production of the cantilever but also by the arrangement of the permanent magnets. In addition, the concept can also be applied to energy harvesters. Beside possible mechanical excitation, the presence of a magnetic stray field alone allows the sensor to convert 20  $\mu\text{T}$  into a power of 1.31  $\mu\text{W}/\text{cm}^3 \cdot \text{Oe}^2$ . The fact that the device does not require any DC bias field makes it very attractive for energy harvesting applications since this allows a purely passive operation. In this manuscript, the sensor assembly, measurements of directional sensitivity, noise level, limit-of-detection, evaluation for energy harvesting applications from magnetic fields and a quantitative sensor model are presented.

## 1. Introduction

### 1.1. Magnetic field sensors

Magnetic field sensors can detect magnetic fields in the range from fT to T [1]. The measurements can be performed contactless and with a high degree of selectivity, resulting in a large scope of applications, such as energy and power, security, electric vehicles, automation, wearables, aerospace, agriculture and geophysics. In the biomedical area, high-sensitivity magnetic field sensors are utilized for the detection of anomalies in the brain or the heart [2,3].

The magnetic device, presented in this paper, can be used as a sensor

as well as an energy harvester. Both types of devices have similar functionalities but exhibit different requirements. In essence, magnetic field sensors usually have the capability to function as magnetic field energy harvesters, but there are some crucial parameters, such as bandwidth, size and directional sensitivity, that have different consequences for sensors and energy harvesters. The process of magnetic field detection by sensors involves the conversion of magnetic fields into electrical signals, which are proportional to each other. Similarly, magnetic field energy harvesters convert magnetic energy into electrical energy, which can be used to power small devices [4]. Magnetic field sensors are designed to detect and measure magnetic fields, while magnetic field energy harvesters are designed to extract and store

\* Corresponding author.

E-mail address: [ra@tf.uni-kiel.de](mailto:ra@tf.uni-kiel.de) (R. Adelung).

<sup>1</sup> These authors contributed equally to this work.

energy from magnetic fields. For magnetic field sensors, a linear response is crucial to establish a direct relation between the magnitude of electrical signals and the corresponding magnetic field amplitude. However, this is not a requirement for energy harvesting applications [5–7].

In the context of a magnetic field sensor, the sensor's ability to detect signals is limited by the presence of noise that arises from mechanical, electrical, or magnetic sources in the surrounding environment. To generate a signal, the sensor converts the magnetic excitations into a mechanical movement (i.e., the bending of the cantilever), which is then translated into an electrical signal. However, there are losses in each step of this conversion process. The limit-of-detection (LoD) refers to the smallest signal that can be detected by the sensor. If the signal is too small, it can be overshadowed by noise and cannot be distinguished. Magnetostrictive materials such as FeCoSiB [8,9] are magnetically soft and can contribute to noise, as small magnetic fields from the surrounding environment can be sufficient to remagnetize them, thereby affecting the measured signal. Changes in magnetization even in small regions or the domain structure can significantly increase the noise in magnetostrictive films. Besides, any noise leading to a mechanical strain of the sensor will contribute to the overall noise, and much effort has been made to reduce the noise in a magnetoelectric (ME) sensor [10,11]. In addition, many sensors require an initialization step to set the magnetic domains to a default state to obtain a reproducible output [12].

It is also necessary that the signal-to-noise ratio (SNR) is high, allowing the detection of very small signals. In addition, a stable, reproducible signal is needed for sensitive measurements. This includes characteristics such as a linear behavior of the output voltage as a function of the applied field amplitudes and the absence of signal drift over time. The supported measurement bandwidth and frequency range should be appropriate for the amplitude spectral density of the corresponding application. Resonant cantilever sensors are typically operated near or at their resonance frequency. Furthermore, the measurement range can be increased by sophisticated readout schemes, e.g., electrical or magnetic modulation [13]. Properties that are advantageous but may not be necessary are a small size of the sensor, no required cooling, high bandwidth and dynamic range, no required additional bias field, a simple readout technique, and a tunable frequency range. These additional qualities will make a sensor stand out in comparison to others with a similar performance [14].

The sensors with the best LoD of 1–10 fT/ $\sqrt{\text{Hz}}$  are SQUIDs and optically pumped magnetometers (OPMs) [15–18]. The downsides to these sensors are the cryogenic cooling for the SQUIDs and the magnetic shielding that is necessary for both sensor types to reach these extreme detection limits [19–22]. Most other sensor concepts have a minimum LoD in the low pT-regime. There are further limitations, such as magnetic noise for fluxgate magnetometers or Hall effect magnetometers, where the sensitivity cannot be brought down further [23].

With the novel sensor concept presented here, an LoD of 46 pT/ $\sqrt{\text{Hz}}$  at 223.5 Hz is reached. Inspired by Elhajjar et al. [24], permanent magnets are used, which have the advantage that magnetic noise is greatly reduced compared to standard magnetostrictive films. In addition to the setup being easy and unaffected by the Earth's magnetic field, it is very tunable to application-specific needs. The field to be measured superposes the magnetic field created by the two opposing magnets and therefore leads to a deflection of the cantilever, which is then readout by a piezoelectric layer.

## 1.2. Energy harvesters

In contrast to sensing, energy harvesting is the process of capturing and storing ambient energy from the environment to be utilized for various applications, such as self-powered sensors and devices or portable electronic devices. Among the various types of ambient energy, mechanical energy has been widely studied as a potential source for energy harvesting. In this context, lead zirconate titanate (PZT), a

ceramic material, has been extensively investigated [4,25,26] due to its high coupling coefficient, which is a measure of the efficiency of the material in converting mechanical energy into electrical energy. However, the mechanical limitations of PZT have led to the examination of alternative materials for energy harvesting, such as polymers and ceramic fiber composites, piezoelectric single crystals, nanostructured ceramics, nanoparticle-polymer composite foams and space-charge electrets.

Polymer-based energy harvesters are mechanically more flexible and have a higher toughness, abrasion resistance, and materials like Polyvinylidene fluoride (PVDF) are promising for biomedical engineering due to their biocompatibility [27]. Ceramic composites have a high strength to weight ratio, are more flexible and are more resistant to environmental degradation. However, both composites still have a comparably low piezoelectric coefficient [26].

The most basic approach for harvesting electrical energy from magnetic fields is by using a coil. Tashiro et al. used Brooks coils and achieved a power density of 1.47  $\mu\text{W}/\text{cm}^3$  in the presence of a magnetic field of approximately 21.2  $\mu\text{T}$  [28]. Liu et al. designed a bimorph piezoelectric cantilever consisting of PZT and two NdFeB magnets attached to the tip, resulting in a power density of 11.73  $\mu\text{W}/\text{cm}^3 \cdot \text{Oe}^2$  for frequencies smaller than 100 Hz and 100  $\mu\text{T}$  [29]. Another method to harvest electrical energy is to combine a piezoelectric material with a magnetostrictive material. The piezoelectric layer is deformed by the magnetostrictive material, which changes shape due to an external magnetic field from the surroundings. It is also possible to combine magnetostrictive films with a proof magnet mass which both contribute to the harvested energy. [30] Ryu et al. demonstrated a device consisting of a piezoelectric fiber and a magnetostrictive Ni plate, which generated 46.3 mW// $\text{cm}^3 \cdot \text{Oe}^2$  at 60 Hz and 160  $\mu\text{T}$  [31]. Recent findings indicate energy harvesting capabilities of 48.68 mW/Oe [32] and 60 mWrms/Oe<sup>2</sup>g<sup>2</sup>cm<sup>3</sup> [33]. The devices have to compromise on magnetic sensitivity, impeding their ability to detect small magnetic fields. Without any modification, the magnetic field sensor with its sensitivity down to 46 pT/ $\sqrt{\text{Hz}}$  is capable of harvesting energies of 1.31  $\mu\text{W}/\text{cm}^3 \cdot \text{Oe}^2$  at a field of 20  $\mu\text{T}$ . In addition, it is possible to drive the sensor acoustically or mechanically.

## 2. Sensor concept

### 2.1. Traditional ME sensors

In contrast to the new concept presented here, conventional magnetoelectric composites consist of a magnetostrictive layer, that transduces a magnetic field into a magnetostrictive strain and a piezoelectric component that transduces a piezoelectric strain into an electrical polarization. This sensor concept was first established by Ryu et al. [34]. The magnitude of the magnetoelectric polarization is determined by the magnetostrictive properties, the mechanical coupling between the two layers, and piezoelectric properties. The electric polarization  $P$ , by a change in the magnetic field  $H$ , depending on the piezoelectric coefficient  $d$ , coupling  $k_c$  and magnetostrictive coefficient  $d^m$  [35], is given as:

$$\frac{\partial P}{\partial H} = dk_c d^m \quad (1)$$

For this sensor Eq. (1) can also be understood in tensor quantities. The realization of such devices was successfully demonstrated by combining macroscopic components with an adhesion layer between the magnetostrictive and piezoelectric component as well as silicon substrate based thin-film technology. The strain  $\varepsilon$  and the distance  $L$  can be related to the ratio of voltage  $U$  and magnetic field  $H$  called sensitivity or magnetoelectric voltage coefficient  $\alpha$  [35].

$$\frac{\partial U}{\partial H} = \alpha = \frac{d}{\varepsilon} k_c d^m L \quad (2)$$

of such devices were found to be 4600 V/T [36] and 7370 kV/T [37] respectively. In addition to the sensitivity, the noise level of a magnetoelectric sensor is important, as both the sensitivity and the noise level are required to determine the detection limit of the sensor, which is a common figure of merit for the performance of a magnetic field sensor, which is 40 pT/ $\sqrt{\text{Hz}}$  [36] and 60 pT/ $\sqrt{\text{Hz}}$  [37] usually for ME sensors.

## 2.2. New concept: hybrid magnetoelectric sensor

The novel sensor concept presents a modified version of an ME sensor that simplifies the design by eliminating the magnetostrictive layer and utilizing opposing permanent magnets to convert the magnetic field into strain in the piezoelectric component. The sensor design is depicted in Fig. 1 and is based on a Si cantilever. One can see the two magnets, one attached to the cantilever and the other one placed 8 mm below. The piezoelectric layer is deposited on top of the silicon. By removing the magnetostrictive layer, the noise sources that are attributed to this layer are also removed, making the sensor more robust. The magnets deflect the cantilever until the repellent forces are in equilibrium with opposing forces originating from gravity or elastic deformation. When superimposed with an additional magnetic field, this equilibrium is disturbed, and consequently, motion is initiated. Thus, a voltage is generated in the piezoelectric layer, which can be detected. The distinctive characteristic is not the addition of permanent magnets, but their utilization for signal generation as further elaborated in the quantitative model.

The elastic deformation of the cantilever can be described by a linear relation between the force and the deflection. The magnetic repulsion decreases by the following proportionality with increasing distance  $R$  between two opposing parallel aligned magnets [38,39]:

$$F \sim 1/R^4 \quad (3)$$

Ideally, a design using freely levitating magnets would be applied, but the instable levitation as described by Earnshaw's theorem [40] does not allow an operation of such a setup. Therefore, as a fixation a cantilever, fixed at one end, is used. The equilibrium distance is determined by displacement, where the forces are compensating for each other. The superposition of the magnetic and elastic force—displacement characteristics results in modified, effective elastic properties. When used in a cantilever design, this can influence the resonance frequency of the sensor while simultaneously increasing the oscillation amplitude, as already observed for the electrostatic interaction of a

cantilever [41]. Another important part is the additional weight the magnet introduces to the cantilever, which will reduce the resonance frequency. Consequently, when used in an ME sensor, this increases the sensitivity of a sensor while shifting the operation frequency to lower regions, which is an improvement of the sensor. Typically, by shifting to lower operational frequencies, the sensitivity would decrease because of an increase in the  $1/f$  noise [42], which would reduce the signal-to-noise ratio. By altering the sensor concept, a shift to a lower operational frequency was possible while also increasing the sensitivity. By choosing silicon technology, the sensor can be easily scaled and integrated by introducing powder permanent magnets [43].

Detecting small magnetic fields is challenging due to the limited signal strength. The signal strength can be improved by operating the sensor in resonance. The lowest resonance frequency of the cantilever is a function of the material properties (in particular, Young's modulus and the mass density), the geometry, and the mass distribution. The geometry and mechanical properties of the cantilever are primarily determined by the substrate material silicon, which is significantly thicker than the other layers (i.e., the electrodes and piezoelectric layer).

## 3. Materials and methods

The sensor is made by using a cantilever with a size of  $25.4 \cdot 2.2 \cdot 0.35 \text{ mm}^3$ , including a piezoelectric layer. This layer material is AlN, fabricated by a sputtering process with a process comparable to [44] and a layer thickness of 1  $\mu\text{m}$ . As a contact pad material, a 150 nm thick layer of Mn was sputter deposited onto the cantilever. A permanent magnet is glued to the bottom of one side of the cantilever with instant adhesive. The magnet is  $5 \cdot 4 \cdot 1 \text{ mm}^3$  in size, made out of Neodymium-iron-boron (NdFeB) by the company Webcraft GmbH, article number Q-05-04-01-N. The contacts are made by wirebonding to a PCB. This PCB is put into a sample holder where the opposing second magnet is placed directly under the first magnet.

## 4. Results

### 4.1. Magnetic characterization

The following measurements and calculations were carried out according to [45], excluding the directional measurement. The typical resonant behavior given by the mechanical resonance is observed in the frequency sweep (cf. Fig. 3). Using a custom-made setup according to

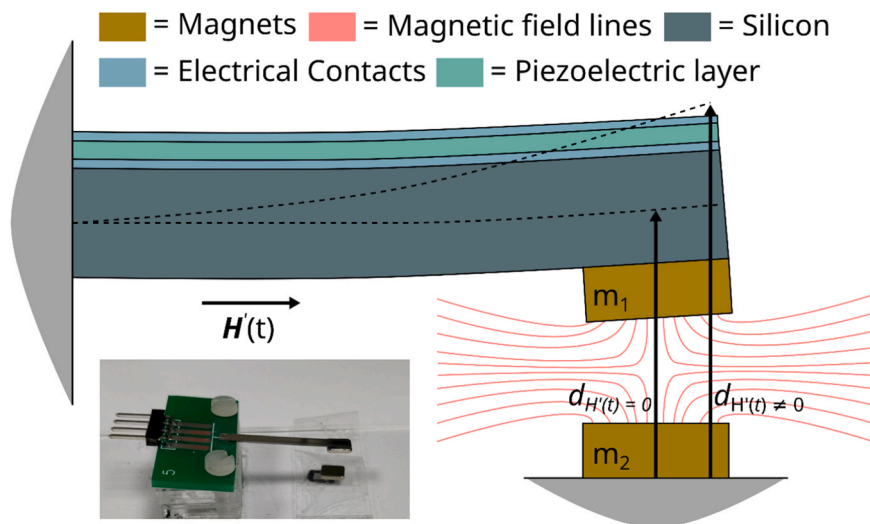


**Fig. 1.** Visualization of the sensor concept (not to scale): The opposing field of the permanent magnets and the combination of the mechanical restoring force and gravitational force of the cantilever are in equilibrium. This leads to a slight upward bending. When a magnetic field  $H(t)$  is applied, the cantilever oscillates. The mechanical stress is translated into an electrical signal within the piezoelectric layer, which can be read out via the electrical contacts.

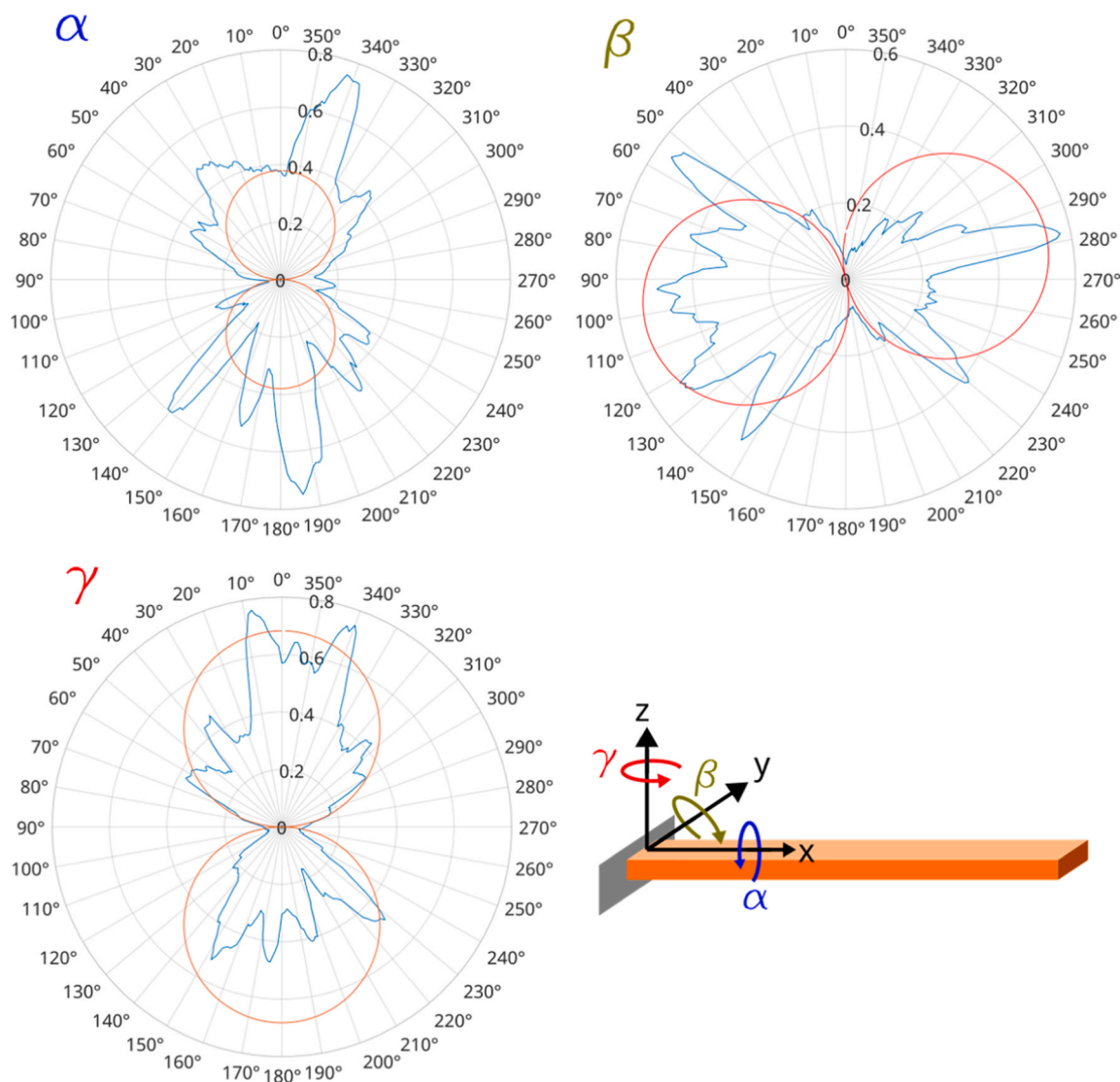


Fig. 2. Directional sensor sensitivity: The sensor response to a magnetic field at a frequency of 227 Hz was measured using a gradient-based evaluation system. Plotted is the linear response for the angles  $\alpha$ ,  $\beta$  and  $\gamma$  as depicted.

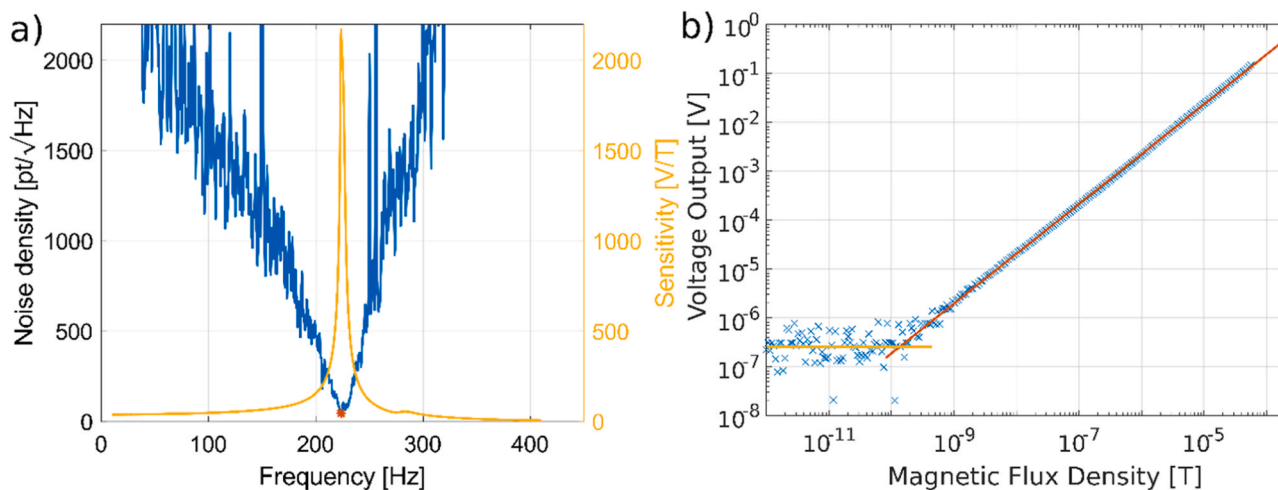


Fig. 3. a) Equalized noise amplitude spectral density and resonant behavior: The equalized noise density and the amplitude depending on the frequency are pictured. b) Input-Output-Amplitude-Relation: The LoD is at 45.88 pT/ $\sqrt{\text{Hz}}$  in resonance. The sensor response is linear up to the detection limit with a sensitivity of 2.2 kV/T.

[46], the sensor was exposed to a homogeneous magnetic field with a constant amplitude of 10  $\mu\text{T}$  at varying frequencies generated by a coil. This setup is lined with acoustic foam and is mechanically decoupled by vibrations dampers, so only magnetic excitation is present and measured [35]. Resonance occurs at 223.5 Hz, with a quality factor of 55 and a 3-dB-bandwidth of 4.1 Hz. The sensitivity within resonance is 2.2 kV/T. The sharp resonance and high-quality factor allow for a better energy storage in the cantilever at resonance because the losses are decreased.

A comprehensive understanding of the sensor's directional characteristics was sought by exposing it to magnetic fields with varying orientations, utilizing a meticulously designed setup comprised of three orthogonal pairs of Helmholtz coils. The sensor's responses at resonance frequency were measured for each discrete direction point, and these values were subsequently normalized with respect to the global maximum. A magnetic field with changing orientation, controlled via a gradient-based evaluation system, is applied to the sensor over a set number of directions. In Fig. 2, the resulting direction dependencies can be seen. In all three directions, there is an axial symmetry. The largest response signal can be gained from the x-direction (where  $\beta = 90^\circ$  and  $\gamma = 0^\circ$ ). Subsequent measurements were conducted in the sensor's longitudinal direction.

When the sensor operates at its mechanical resonance, the equalized noise amplitude spectral density is minimized. In resonance at 223.5 Hz the noise density is the lowest and the sensitivity is the highest. Outside the resonance, the amplitude of noise density becomes larger, resulting in a decrease in the signal-to-noise ratio. This is because the signal power is reduced outside the resonance due to the lower available sensitivity. In Fig. 3b, the Input-Output-Amplitude-Relation of the sensor in resonance is shown. The measurement is performed by applying an alternating magnetic field with decreasing amplitude at the resonance frequency [43]. The resonance frequency is selected because it offers the highest available sensor sensitivity. From Fig. 3b, the LoD can be determined, which is approximately 45.88 pT/ $\sqrt{\text{Hz}}$  for this specific sensor. Furthermore, it can be observed that a linear amplitude relationship between magnetic flux density and sensor output voltage is supported until nearly 100  $\mu\text{T}$ .

Additionally, further measurements were conducted with both increasing and decreasing DC magnetic bias fields to investigate any potential magnetic hysteresis behavior of the sensor. By design, the hysteresis behavior influenced by the magnetic domains should be negligible for this sensor concept. Ultimately, the empirical results demonstrated a nearly linear behavior up to 1 mT, with negligible values compared to the signal output in resonance, which is approximately 0.6 V/T (see supplementary Fig. A.1). This is the tested range, and it could be negligible for even higher applied fields.

#### 4.2. Model

We consider the system displayed in Fig. 1. The loading by force  $\bar{F}$  and torque  $\bar{T}$  (cf. supplementary, Fig. B1) results from the interaction of the two permanent magnets and the applied magnetic field  $\mathbf{H}'(t)$ . The main quantity of interest is the beam deflection  $w(x_1, t)$ . We can compute other quantities, such as strain  $\epsilon$  and voltage  $u$  in the piezoelectric layer, as dependent quantities. To reduce the complexity of the considered system, we introduce the following simplifications and assumptions.

First, we replace each permanent magnet with a magnetically equivalent magnetic dipole moment  $\mathbf{m}_1$  resp.  $\mathbf{m}_2$  with norm  $\|\mathbf{m}_i\| = M$ . The magnitude  $M = B_r V / \mu_0$  is computed from the remanence  $B_r$  and volume  $V$  of the permanent magnet. The dipole  $\mathbf{m}_2$  is assumed to remain fixed in orientation, while the dipole  $\mathbf{m}_1$  moves and tilts according to the beam deflection. In the mechanical sense, we replace the permanent magnet attached to the beam by the point mass  $m$ . Furthermore, we adopt Bernoulli beam theory [47] and assume pure bending with small deflection  $w(x_1, t)$ . Mechanically, the piezoelectric thin-film is neglected. The fixed end support as well as the aforementioned assumptions imply

the following boundary conditions for the beam deflection  $w(x_1, t)$ :

$$w(x_1 = 0) = 0 \quad (4)$$

$$\frac{\partial w}{\partial x_1}(x_1 = 0) = 0 \quad (5)$$

$$\frac{\partial^2 w}{\partial x_1^2}(x_1 = a) = -\frac{\bar{T}_2}{EI} = \frac{\mu_0 M}{EI} \left( H(t) + \frac{M}{2\pi(d_0 - w(a))^3} \frac{\partial w}{\partial x_1}(x_1 = a) \right) \quad (6)$$

$$\frac{\partial^3 w}{\partial x_1^3}(x_1 = a) = -\frac{\bar{F}_3}{EI} = \frac{3\mu_0 M^2}{2\pi EI(d_0 - w(a))^4} + \frac{m}{EI} \ddot{w}(x_1 = a). \quad (7)$$

The force and torque boundary conditions at the free end result from the point mass  $m$  and the magnetic interaction of the dipoles  $\mathbf{m}_1$  and  $\mathbf{m}_2$  as well as the applied magnetic field  $\mathbf{H}'(t)$ . The governing partial differential equation reads:

$$EI \frac{\partial^4 w}{\partial x_1^4} + \rho A \frac{\partial^2 w}{\partial t^2} + \eta \frac{\partial w}{\partial t} = 0, \quad (8)$$

cf. [48], where  $E$  denotes Young's modulus,  $I = bc^3/12$  represents the area moment of inertia,  $\rho$  is the mass density,  $A = bc$  denotes the cross-sectional area and  $\eta$  summarizes all damping effects. We compute the solution using the Ritz-Galerkin method; see appendix B.

In the following, we choose for the test function

$$g(x_1) = \delta g(x_1) = x_1^2, \quad (9)$$

cf. supplementary B. Furthermore, we choose the parameter set displayed in the supplementary Tab. B.1. In particular, we use the damping parameter  $\eta$  to fit the piezoelectric voltage in resonance to experimental data.

## 5. Discussion

### 5.1. Magnetic characterization

The presented cantilever sensor exhibits standard resonance behavior as anticipated when exposed to a magnetic field. The empirically determined resonance frequency is at 223.5 Hz. By altering the size of the magnets or introducing additional weights to the cantilever, this frequency can be adjusted, enabling the sensor to be utilized in a frequency range appropriate for biomedical applications. Due to the asymmetric geometry of the cantilever itself and the magnets used, there is an asymmetric response to magnetic fields depending on the direction. The sample alignment is not guaranteed to be perfect; therefore, a slight tilt may have occurred during the directional characterization process. The sensor exhibits a directional dependency and is most sensitive when the field is applied longitudinally along the direction of the cantilever. This can be attributed to the geometry of the repelling magnetic field, whereby the superposition of fields from different directions results in varying deflections of the cantilever. This property inherently enables the sensor to directionally "filter" magnetic fields originating from directions other than the field of interest. If multiple sensors are used, a directional resolution might be achievable.

In mechanical resonance, the equalized noise amplitude spectral density is typically minimized due to the high available sensitivity. The enhancement in resonance serves to amplify the desired magnetic signal, while the noise amplitude spectral density remains constant within this narrow bandwidth. The increased signal-to-noise ratio in the vicinity of the resonance frequency enables more accurate measurements and detection of the target magnetic signal, ultimately improving the overall performance of the system.

Despite its simplicity, the sensor can compete with other magneto-electric sensors that have detection limits of 70 pT/ $\sqrt{\text{Hz}}$  at 10 Hz [44], 350 pT/ $\sqrt{\text{Hz}}$  at 25 Hz [49], 72 pT/ $\sqrt{\text{Hz}}$  at 10 kHz [50], and 60 pT/ $\sqrt{\text{Hz}}$

[37]. The sensor has a bandwidth that allows to detect amplitude spectral densities starting at  $46 \text{ pT}/\sqrt{\text{Hz}}$  and higher. Its robustness is particularly noteworthy in the presence of DC magnetic fields, with changes in voltage output of only approximately  $30 \text{ mV/T}$  observed even in the presence of fields as large as  $\pm 10 \text{ mT}$ . The sensitivity of the sensor itself is at  $2.2 \text{ kV/T}$ . There are recent publications about ME sensors with a lower LoD such [51–54] with e.g.,  $0.9 \text{ pT}/\sqrt{\text{Hz}}$  and  $0.05 \text{ pT}/\sqrt{\text{Hz}}$  as the lowest values. In contrast to the device presented here these sensors have various drawbacks, e.g., requirement of magnetic or electric biasing, higher complexity, lower sensitivity and lower robustness to large magnetic fields in particular earth's magnetic field.

Other publications with more simple designs and other unique features like a high flexibility or a reduced power consumption have a higher LoD of  $115 \text{ pT}$  and  $200 \text{ pT}$  [55,56]. All in all, there seems to be a tradeoff between a low LoD and unique sensor features or a simple design and fabrication process. The here presented concept represents a balance of a remarkable low LoD, accompanied by low complexity, bias-free characteristics, power efficiency and exceptional robustness.

The performance results of the sensor demonstrate that the concept of employing a cantilever-based sensor that incorporates fixed permanent magnets is effective across a wide range of magnetic fields. The concept of magnetic field detection by the set of magnets without any further magnetostrictive components is applicable. This design strategy offers a promising approach for sensitive and robust magnetic field detection, making it a viable option for various applications that require such capabilities.

By using silicon technology, the sensor can be directly used in integrated circuits, which should limit the noise even further because of the shorter connection ways, and the device is built as one from the beginning. The macroscopic magnets could be replaced by MEMS-compatible powder magnets, which may be rather simple because of the elementary character of only using two magnets [43]. Another benefit is that no active bias field or magnetostrictive layer is needed, which makes the concept simpler and more robust and the fabrication process easier. Overall, the sensor shows remarkable performance. It not only has a comparable or better detection limit than other ME sensors but also offers more options to tune the resonance frequency, needs fewer components, which must be manufactured in a clean room, and has fewer noise sources. Other readout schemes can be applied, such as a piezotronic readout for sensor usage or electret or readout using Triboelectric Nanogenerators (TEGs) for energy harvesting usage [57].

## 5.2. Energy harvesting capabilities

In addition, the sensor exhibits energy harvesting capabilities because it can convert a magnetic field into electric energy, which is the readout method of the sensor. It is also possible to drive the sensor mechanically due to its high weight or by vibrations or acoustic excitation, which offers the possibility of converting different forms of energy into electrical energy. Tashiro et al. and Roscoe et al. calculated the power density at magnetic fields of approximately  $20 \text{ } \mu\text{T}$  [28,58]. At these fields, the piezoelectric crystal creates a voltage of  $30 \text{ mV}$ . With an input resistance of  $470 \text{ k}\Omega$  and an effective volume of  $0.104 \text{ cm}^3$ , this translates to a power density of  $1.31 \text{ } \mu\text{W}/\text{cm}^3 \cdot \text{Oe}^2$ . Fig. A.2 in the supplementary materials presents a comprehensive series of resistors that have been employed to determine the optimal external load. For the volume, the silicon cantilever as well as the permanent magnet are considered. The piezoelectric layer as well as the magnetostrictive layer are neglected for the calculation. This shows that in comparison to conventional energy harvesters, the sensor has a comparably low power density output. This is because the sensing and not the energy harvesting capabilities are optimized. In addition, the dynamic range covers a significant regime. These two features can be combined, to operate the sensor autonomously. Besides, the volume could be optimized e.g., the substrate or size of the magnets which could lead to a higher normalized power density output.

## 5.3. Model

The resulting piezoelectric voltage amplitude as a function of frequency, calculated by using the presented model, is displayed in Fig. 4. The shape of the frequency response matches the experimental findings, and we are easily able to adapt the model to conform with the experimental voltage in resonance. The model predicts resonance at  $210.1 \text{ Hz}$ , which is in reasonably agreement with the empirically determined value of  $223.5 \text{ Hz}$ .

Subsequently, we can study qualitative trends with respect to parameter variations and initiate ideas for further design changes. In Fig. 4 and Fig. B.2, we showcase the piezoelectric voltage amplitude as a function of frequency with multiple parameter variations.

For the detection of biomagnetic signals, a high voltage amplitude at a small resonance frequency is desirable. We observe that all investigated parameter variations influence both the resonance frequency and the voltage amplitude in resonance. In particular, we observe that with some parameter variations (e.g., dipole magnitude  $M$  and cantilever length  $a$ , cf. Fig. B.2), we are able to decrease the resonance frequency while we have to accept a simultaneous decrease in voltage. With other parameter variations (e.g., Young's modulus  $E$ , cantilever height  $c$  and point mass  $m$ ), we are able to fulfill both objectives at the same time (decrease resonance frequency, increase voltage amplitude). Hence, the latter class of parameters is particularly suited to improve the sensor performance.

We can draw another conclusion from Fig. 4 and Fig. B.2 concerning the merit, which can be gained from a certain parameter variation. For some parameters (e.g.,  $a$  and  $c$ ), we can obtain a strong variation in resonance frequency with a proportionately small change in parameter. On the other hand, a strong variation in voltage can be achieved by a proportionately small change of  $M$  and  $a$ . Thus, certain parameters are suitable tools to influence the resonance frequency, while others lend themselves particularly well to influencing the voltage output.

## 5.4. Outlook

By varying the parameters, it should be possible to improve the sensor characteristics further. Some variations, like magnet distance, magnet displacement and magnet strength, were tested. The most promising result up to now is achieved by replacing the bottom magnet with a smaller one, c.f. Fig. 5. The output amplitude is increased in the asymmetric configuration. The limit of detection in that case is similar at least to the previously presented values and can seemingly reach low pT-range values.

In particular, the amplitude increase in the resonant sweep is an advantage for energy harvester applications because it leads to higher energy output. This means, that the observed effect is advantageous for both sensor and energy harvester. The signal strength can be increased while the LoD also decreases, which indicates that the noise did not increase proportional to the signal output amplitude.

## 6. Conclusions

The proposed new magnetic field sensor concept within this contribution shows a limit-of-detection of approximately  $46 \text{ pT}/\sqrt{\text{Hz}}$  at a determined resonance frequency of  $223.5 \text{ Hz}$ . The underlying mechanism is based on the superposition of the magnetic field to be measured and the opposing field of the permanent magnets of the sensor.

The flexible, simple sensor design allows for easy adaptation of the sensor properties, e.g., the resonance frequency and bandwidth, which makes it a promising candidate for a wide range of applications. The distance of the magnets, their alignment, their strength, or the magnet geometry could be varied to name some of the possible adjustments.

The sensor is not significantly influenced by magnetic bias fields up to  $\pm 1 \text{ mT}$  (cf. supplementary Fig. A.1), and it does not need special shielding, as many other magnetic field sensors do. It is robust, does not

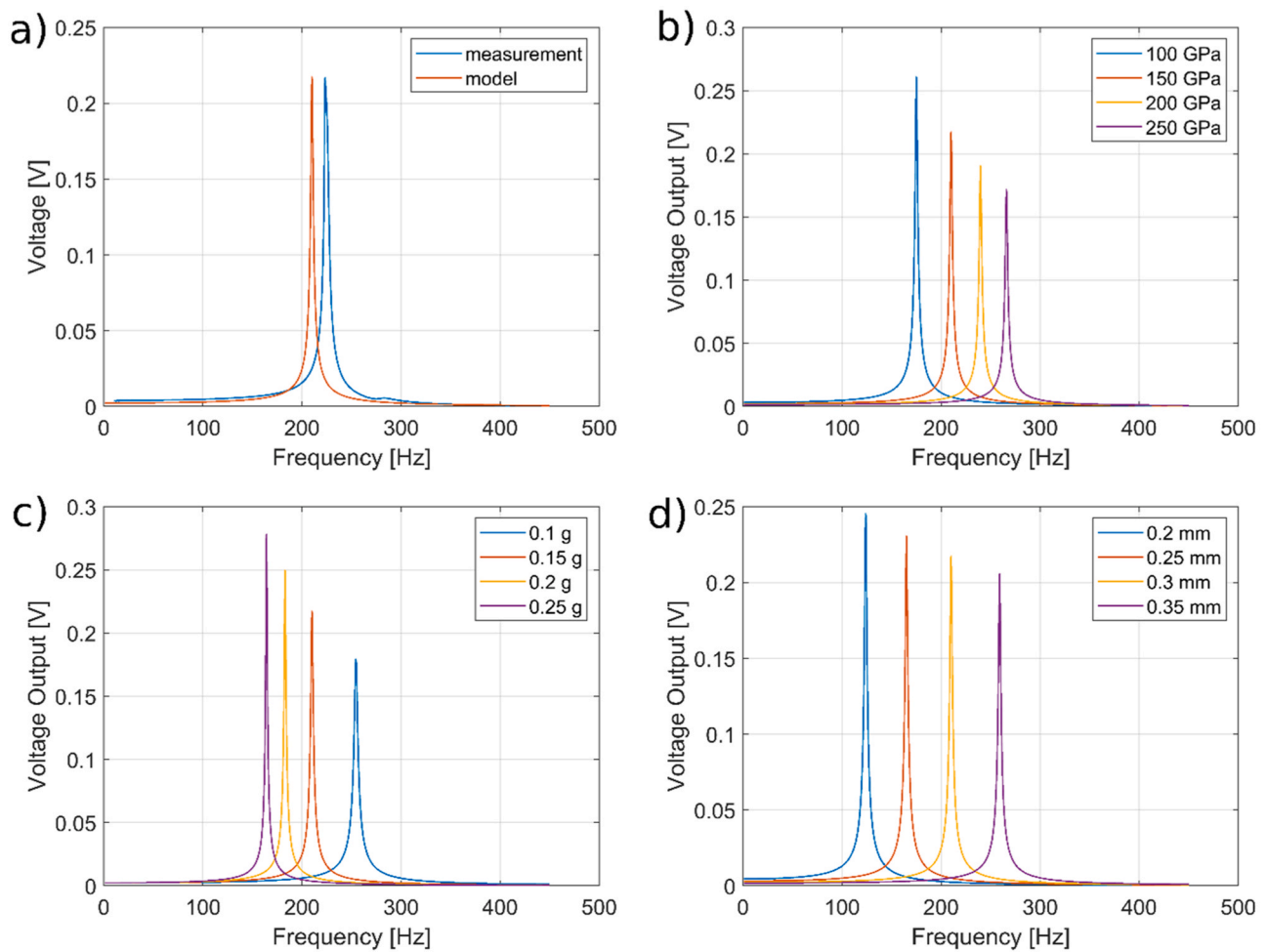


Fig. 4. Measured and modelled frequency behavior: a) Piezoelectric voltage amplitude as a function of frequency derived from the model in comparison to the measured frequency sweep. b-d) Modelled parameter variations for b) Young's modulus, c) point mass and d) cantilever height.

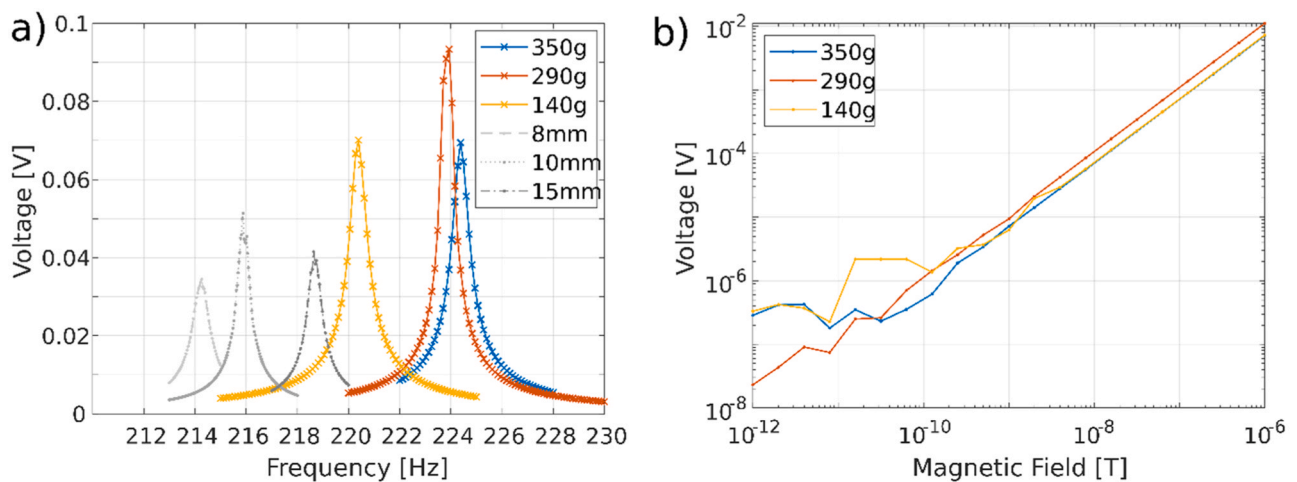


Fig. 5. Influence of different magnets: a) Resonance behavior is depicted for parameter variations (with a factor 10 lower excitation field in comparison to the other measurements). Those with an asymmetric magnet, depicted using colors, have the highest amplitude. The gray curves are resonance behaviors for distance variations of the magnets. The magnetic adhesive force is given in weight in the legend which is equivalent to 3.43 N, 2.84 N and 1.37 N, respectively. b) Input-Output-Amplitude-Relation for different asymmetric magnet configurations where the bottom magnet is changed.

show a significant drift and can measure small fields. Due to the piezoelectric layer, different readout techniques can be used. There are several application possibilities; for example, it could be used in MEMS

technology or as an energy harvester.

Additionally, an analytical solution for a magnetic field sensor was presented. The model is able to capture important experimental results

such as the piezoelectric voltage amplitude in resonance, the shape of the frequency response and the resonance frequency. Hence, the system is well-understood and mainly determined by the modeled phenomena.

### CRedit authorship contribution statement

**Martha Gerhardt:** Conceptualization, Validation, Investigation, Writing – original draft, Visualization, Project administration. **Lukas Zimoch:** Conceptualization, Validation, Investigation, Writing – original draft, Visualization, Project administration. **Christian Dorn:** Methodology, Writing – original draft, Visualization. **Eric Elzenheimer:** Validation, Investigation, Writing – review & editing. **Christin Bald:** Writing – review & editing. **Tjorben Lerg:** Investigation, Writing – review & editing. **Johannes P. Hoffmann:** Writing – review & editing. **Sören Kaps:** Conceptualization, Software, Validation, Writing – original draft. **Michael Höft:** Writing – review & editing. **Gerhard Uwe Schmidt:** Writing – review & editing. **Stephan Wulfinghoff:** Methodology, Writing – review & editing. **Rainer Adelung:** Conceptualization, Writing – review & editing, Supervision.

### Declaration of Competing Interest

The authors declare that they have no known competing financial interests or personal relationships that could have appeared to influence the work reported in this paper.

### Data availability

Data will be made available on request.

### Acknowledgement

This work was supported by the German Research Foundation (Deutsche Forschungsgemeinschaft, DFG) under project 286471992 (Collaborative Research Centre 1261, “Magnetolectric Sensors: From Composite Materials to Biomagnetic Diagnostics”). We thank Henrik Wolfram for helping with the directional characterization setup and Hanna Lewitz and Lars Thormählen for providing the cantilevers.

### Appendix A. Supporting information

Supplementary data associated with this article can be found in the online version at [doi:10.1016/j.nanoen.2023.108720](https://doi.org/10.1016/j.nanoen.2023.108720).

### References

- A.L. Herrera-May, L.A. Aguilera-Cortés, P.J. García-Ramírez, E. Manjarrez, Resonant magnetic field sensors based On MEMS technology, *Sensors* 9 (2009) 7785–7813, <https://doi.org/10.3390/s91007785>.
- J. Lenz, S. Edelstein, Magnetic sensors and their applications, *IEEE Sens. J.* 6 (2006) 631–649, <https://doi.org/10.1109/JSEN.2006.874493>.
- E. Elzenheimer, P. Hayes, L. Thormählen, E. Engelhardt, A. Zaman, E. Quandt, N. Frey, M. Höft, G. Schmidt, Investigation of Converse magnetolectric thin-film sensors for magnetocardiography, *IEEE Sens. J.* 23 (2023) 5660–5669, <https://doi.org/10.1109/JSEN.2023.3237910>.
- Q. Zheng, B. Shi, Z. Li, Z.L. Wang, Recent progress on piezoelectric and triboelectric energy harvesters in biomedical systems, *Adv. Sci.* 4 (2017), 1700029, <https://doi.org/10.1002/adv.201700029>.
- S. Roundy, P.K. Wright, J. Rabaey, A study of low level vibrations as a power source for wireless sensor nodes, *Comput. Commun.* 26 (2003) 1131–1144, [https://doi.org/10.1016/S0140-3664\(02\)00248-7](https://doi.org/10.1016/S0140-3664(02)00248-7).
- S. Pattipaka, J. Jeong, H. Choi, J. Ryu, G.-T. Hwang, Magneto-mechano-electric (MME) composite devices for energy harvesting and magnetic field sensing applications, *Sensors* 22 (2022), <https://doi.org/10.3390/s22155723>.
- K.-H. Cho, C.-S. Park, S. Priya, Effect of intensive and extensive loss factors on the dynamic response of magnetolectric laminates, *Appl. Phys. Lett.* 97 (2010), 182902, <https://doi.org/10.1063/1.3511285>.
- A.P. Thomas, M. Gibbs, Anisotropy and magnetostriction in metallic glasses, *J. Magn. Magn. Mater.* 103 (1991/1992) 97–110, [https://doi.org/10.1016/0304-8853\(92\)90242-G](https://doi.org/10.1016/0304-8853(92)90242-G).
- P. Hayes, V. Schell, S. Salzer, D. Burdin, E. Yaras, A. Piorra, R. Knöchel, Y. K. Fetisov, E. Quandt, Electrically modulated magnetolectric AlN/FeCoSiB film composites for DC magnetic field sensing, *J. Phys. D Appl. Phys.* 51 (2018), 354002, <https://doi.org/10.1088/1361-6463/aad456>.
- Y.J. Wang, J.Q. Gao, M.H. Li, Y. Shen, D. Hasanyan, J.F. Li, D. Viehland, A review on equivalent magnetic noise of magnetolectric laminate sensors, *Philos. Trans. A Math. Phys. Eng. Sci.* 372 (2014), 20120455, <https://doi.org/10.1098/rsta.2012.0455>.
- Z.Q. Lei, G.J. Li, W.F. Egelhoff, P.T. Lai, P.W.T. Pong, Review of noise sources in magnetic tunnel junction sensors, *IEEE Trans. Magn.* 47 (2011) 602–612, <https://doi.org/10.1109/TMAG.2010.2100814>.
- J. Baumann, D. Göger, U. Kiencke, A magneto-elastic sensor for measuring pressure oscillations in common rail systems, *IFAC Proc.* 38 (2005) 67–72, <https://doi.org/10.3182/20050703-6-CZ-1902.01899>.
- J. Reermann, S. Zabel, C. Kirchhof, E. Quandt, F. Faupel, G. Schmidt, Adaptive readout schemes for thin-film magnetolectric sensors based on the delta-E effect, *IEEE Sens. J.* 16 (2016) 4891–4900, <https://doi.org/10.1109/JSEN.2016.2553962>.
- M. Bichurin, R. Petrov, O. Sokolov, V. Leontiev, V. Kuts, D. Kiselev, Y. Wang, Magnetolectric magnetic field sensors: a review, *Sensors* 21 (2021), <https://doi.org/10.3390/s21186232>.
- W. Li, X. Peng, S. Li, C. Liu, H. Guo, P. Lin, W. Zhang, Unshielded scalar magnetometer based on nonlinear magneto-optical rotation with amplitude modulated light, in: *Proceedings of the IEEE International Frequency Control Symposium (IFCS)*, New Orleans, LA, USA, IEEE, 2016, 1–4.
- S.-Q. Liang, G.-Q. Yang, Y.-F. Xu, Q. Lin, Z.-H. Liu, Z.-X. Chen, Simultaneously improving the sensitivity and absolute accuracy of CPT magnetometer, *Opt. Express* 22 (2014) 6837–6843, <https://doi.org/10.1364/OE.22.006837>.
- K. Sternickel, A.I. Braginski, Biomagnetism using SQUIDs: status and perspectives, *Supercond. Sci. Technol.* 19 (2006) S160–S171, <https://doi.org/10.1088/0953-2048/19/3/024>.
- M. Buchner, K. Höfler, B. Henne, V. Ney, A. Ney, Tutorial: basic principles, limits of detection, and pitfalls of highly sensitive SQUID magnetometry for nanomagnetism and spintronics, *J. Appl. Phys.* 124 (2018), 161101, <https://doi.org/10.1063/1.5045299>.
- J. Wang, K. Yang, R. Yang, X. Kong, W. Chen, SQUID gradiometer module for fetal magnetocardiography measurements inside a thin magnetically shielded room, *IEEE Trans. Appl. Supercond.* 29 (2019) 1–4, <https://doi.org/10.1109/TASC.2018.2889865>.
- Y.P. Pan, S.Y. Wang, X.Y. Liu, Y.S. Lin, L.X. Ma, Y. Feng, Z. Wang, L. Chen, Y. H. Wang, 3D nano-bridge-based SQUID susceptometers for scanning magnetic imaging of quantum materials, *Nanotechnology* 30 (2019), 305303, <https://doi.org/10.1088/1361-6528/ab1792>.
- D. Sheng, A.R. Perry, S.P. Krzyzewski, S. Geller, J. Kitching, S. Knappe, A microfabricated optically-pumped magnetic gradiometer, *Appl. Phys. Lett.* 110 (2017) 31106, <https://doi.org/10.1063/1.4974349>.
- G. Zhang, S. Huang, Q. Lin, Magnetoencephalography using a compact multichannel atomic magnetometer with pump-probe configuration, *AIP Adv.* 8 (2018), 125028, <https://doi.org/10.1063/1.5066604>.
- D. Murzin, D.J. Mapps, K. Levada, V. Belyaev, A. Omelyanchik, L. Panina, V. Rodionova, Ultrasensitive magnetic field sensors for biomedical applications, *Sensors* 20 (2020), <https://doi.org/10.3390/s20061569>.
- R. Elhajjar, C.-T. Law, A. Pegoretti, Magnetostrictive polymer composites: recent advances in materials, structures and properties, *Prog. Mater. Sci.* 97 (2018) 204–229, <https://doi.org/10.1016/j.pmatsci.2018.02.005>.
- V. Annapureddy, H. Palneedi, G.-T. Hwang, M. Peddigari, D.-Y. Jeong, W.-H. Yoon, K.-H. Kim, J. Ryu, Magnetic energy harvesting with magnetoelastics: an emerging technology for self-powered autonomous systems, *Sustain. Energy Fuels* 1 (2017) 2039–2052, <https://doi.org/10.1039/C7SE00403F>.
- H.S. Kim, J.-H. Kim, J. Kim, A review of piezoelectric energy harvesting based on vibration, *Int. J. Precis. Eng. Manuf.* 12 (2011) 1129–1141, <https://doi.org/10.1007/s12541-011-0151-3>.
- M. Habib, I. Lantgios, K. Hornbostel, A review of ceramic, polymer and composite piezoelectric materials, *J. Phys. D Appl. Phys.* 55 (2022), 423002, <https://doi.org/10.1088/1361-6463/ac8687>.
- K. Tashiro, H. Wakiwaka, S. Inoue, Y. Uchiyama, Energy harvesting of magnetic power-line noise, *IEEE Trans. Magn.* 47 (2011) 4441–4444, <https://doi.org/10.1109/TMAG.2011.2158190>.
- G. Liu, P. Ci, S. Dong, Energy harvesting from ambient low-frequency magnetic field using magneto-mechano-electric composite cantilever, *Appl. Phys. Lett.* 104 (2014) 32908, <https://doi.org/10.1063/1.4862876>.
- M.G. Kang, R. Sriramdas, H. Lee, J. Chun, D. Maurya, G.T. Hwang, J. Ryu, S. Priya, High power magnetic field energy harvesting through amplified magneto-mechanical vibration, *Adv. Energy Mater.* 8 (2018), 1703313, <https://doi.org/10.1002/aenm.201703313>.
- J. Ryu, J.-E. Kang, Y. Zhou, S.-Y. Choi, W.-H. Yoon, D.-S. Park, J.-J. Choi, B.-D. Hahn, C.-W. Ahn, J.-W. Kim, Y.-D. Kim, S. Priya, S.Y. Lee, S. Jeong, D.-Y. Jeong, Ubiquitous magneto-mechano-electric generator, *Energy Environ. Sci.* 8 (2015) 2402–2408, <https://doi.org/10.1039/C5EE00414D>.
- L. Hu, H. Wu, Q. Zhang, H. You, J. Jiao, H. Luo, Y. Wang, A. Gao, C. Duan, Self-powered energy-harvesting magnetic field sensor, *Appl. Phys. Lett.* 120 (2022) 43902, <https://doi.org/10.1063/5.0079709>.
- Z. Yu, J. Yang, J. Cao, L. Bian, Z. Li, X. Yuan, Z. Wang, Q. Li, S. Dong, A PMNN-PZT piezoceramic based magneto-mechano-electric coupled energy harvester, *Adv. Funct. Mater.* 32 (2022), 2111140, <https://doi.org/10.1002/adfm.202111140>.
- J. Ryu, S. Priya, K. Uchino, H.E. Kim, Magnetolectric Effect in Composites of Magnetostrictive and Piezoelectric Materials (2002).

- [35] A. Piorra, R. Jahns, I. Teliban, J.L. Gugat, M. Gerken, R. Knöchel, E. Quandt, Magnetolectric thin film composites with interdigital electrodes, *Appl. Phys. Lett.* 103 (2013) 32902, <https://doi.org/10.1063/1.4812706>.
- [36] J. Zhai, Z. Xing, S. Dong, J. Li, D. Viehland, Magnetolectric laminate composites: an overview, *J. Am. Ceram. Soc.* 91 (2008) 351–358, <https://doi.org/10.1111/j.1551-2916.2008.02259.x>.
- [37] J. Su, F. Niekieł, S. Fichtner, L. Thormaehlen, C. Kirchhof, D. Meyners, E. Quandt, B. Wagner, F. Lofink, AlScN-based MEMS magnetolectric sensor, *Appl. Phys. Lett.* 117 (2020), 132903, <https://doi.org/10.1063/5.0022636>.
- [38] Y. Kraftmakher, Magnetic field of a dipole and the dipole–dipole interaction, *Eur. J. Phys.* 28 (2007) 409–414, <https://doi.org/10.1088/0143-0807/28/3/003>.
- [39] J.G. Ku, X.Y. Liu, H.H. Chen, R.D. Deng, Q.X. Yan, Interaction between two magnetic dipoles in a uniform magnetic field, *AIP Adv.* 6 (2016) 25004, <https://doi.org/10.1063/1.4941750>.
- [40] L. Tonks, Note on Earnshaw's theorem, *Electr. Eng.* 59 (1940) 118–119, <https://doi.org/10.1109/EE.1940.6434810>.
- [41] M. Mintken, M. Schweichel, S. Schröder, S. Kaps, J. Carstensen, Y.K. Mishra, T. Strunskus, F. Faupel, R. Adelung, Nanogenerator and piezotronic inspired concepts for energy efficient magnetic field sensors, *Nano Energy* 56 (2019) 420–425, <https://doi.org/10.1016/j.nanoen.2018.11.031>.
- [42] F.N. Hooge, T.G.M. Kleinpenning, L.K.J. Vandamme, *Experimental studies on 1/f noise* 1981, *Rep. Prog. Phys.* (1981).
- [43] F. Niekieł, J. Su, M.T. Bodduluri, T. Lisec, L. Blohm, I. Pieper, B. Wagner, F. Lofink, Highly sensitive MEMS magnetic field sensors with integrated powder-based permanent magnets, *Sens. Actuators A Phys.* 297 (2019), 111560, <https://doi.org/10.1016/j.sna.2019.111560>.
- [44] P. Hayes, M. Jovičević Klug, S. Toxværd, P. Durdaut, V. Schell, A. Teplyuk, D. Burdin, A. Winkler, R. Weser, Y. Fetisov, M. Höft, R. Knöchel, J. McCord, E. Quandt, Converse magnetolectric composite resonator for sensing small magnetic fields, *Sci. Rep.* 9 (2019) 16355, <https://doi.org/10.1038/s41598-019-52657-w>.
- [45] E. Elzenheimer, C. Bald, E. Engelhardt, J. Hoffmann, P. Hayes, J. Arbutini, A. Bahr, E. Quandt, M. Höft, G. Schmidt, Quantitative evaluation for magnetolectric sensor systems in biomagnetic diagnostics, *Sensors* 22 (2022), <https://doi.org/10.3390/s22031018>.
- [46] R. Jahns, R. Knochel, H. Greve, E. Woltermann, E. Lage, E. Quandt, Magnetolectric sensors for biomagnetic measurements, in: *Proceedings of the IEEE International Symposium on Medical Measurements and Applications, Bari, Italy, IEEE, 2011, 107–110*.
- [47] E. Carrera, G. Giunta, M. Petrolo, *Beam structures: Classical and Advanced Theories*, Wiley, Chichester West Sussex U.K, 2011.
- [48] R.W. Clough, J. Penzien, *Dynamics of structures*, second. ed. revised., Computers and Structures, Berkeley, 2003.
- [49] B. Spetzler, C. Bald, P. Durdaut, J. Reermann, C. Kirchhof, A. Teplyuk, D. Meyners, E. Quandt, M. Höft, G. Schmidt, F. Faupel, Exchange biased delta-E effect enables the detection of low frequency pT magnetic fields with simultaneous localization, *Sci. Rep.* 11 (2021) 5269, <https://doi.org/10.1038/s41598-021-84415-2>.
- [50] J.M. Meyer, V. Schell, J. Su, S. Fichtner, E. Yasar, F. Niekieł, T. Giese, A. Kittmann, L. Thormaehlen, V. Lebedev, S. Moench, A. Žukauskaitė, E. Quandt, F. Lofink, Thin-film-based SAW magnetic field sensors, *Sensors* 21 (2021), <https://doi.org/10.3390/s21248166>.
- [51] M. Peddigari, K. Woo, S.-D. Kim, M.S. Kwak, J.W. Jeong, J.-H. Kang, S.-H. Lee, J. H. Park, K.-I. Park, V. Annapureddy, J. Jang, Y. Min, C.-W. Ahn, J.-J. Choi, B.-D. Hahn, W.-H. Yoon, J. Ryu, G.-T. Hwang, Ultra-magnetic field sensitive magnetolectric composite with sub-pT detection limit at low frequency enabled by flash photon annealing, *Nano Energy* 90 (2021), 106598, <https://doi.org/10.1016/j.nanoen.2021.106598>.
- [52] V. Annapureddy, H. Palneedi, W.-H. Yoon, D.-S. Park, J.-J. Choi, B.-D. Hahn, C.-W. Ahn, J.-W. Kim, D.-Y. Jeong, J. Ryu, A pT/√Hz sensitivity ac magnetic field sensor based on magnetolectric composites using low-loss piezoelectric single crystals, *Sens. Actuators A Phys.* 260 (2017) 206–211, <https://doi.org/10.1016/j.sna.2017.04.017>.
- [53] M. Oogane, K. Fujiwara, A. Kanno, T. Nakano, H. Wagatsuma, T. Arimoto, S. Mizukami, S. Kumagai, H. Matsuzaki, N. Nakasato, Y. Ando, Sub-pT magnetic field detection by tunnel magneto-resistive sensors, *Appl. Phys. Express* 14 (2021), 123002, <https://doi.org/10.35848/1882-0786/ac3809>.
- [54] P.T. Das, H. Nhalil, M. Schultz, S. Amrusi, A. Grosz, L. Klein, Detection of low-frequency magnetic fields down to sub-pT resolution with Planar-Hall effect sensors, *IEEE Sens. Lett.* 5 (2021) 1–4, <https://doi.org/10.1109/LSENS.2020.3046632>.
- [55] N. Yang, H. Wu, S. Wang, G. Yuan, J. Zhang, O. Sokolov, M.I. Bichurin, K. Wang, Y. Wang, Ultrasensitive flexible magnetolectric sensor, *APL Mater.* 9 (2021) 21123, <https://doi.org/10.1063/5.0039089>.
- [56] Z. Chu, C. Dong, C. Tu, X. Liang, H. Chen, C. Sun, Z. Yu, S. Dong, N.-X. Sun, A low-power and high-sensitivity magnetic field sensor based on converse magnetolectric effect, *Appl. Phys. Lett.* 115 (2019), 162901, <https://doi.org/10.1063/1.5122774>.
- [57] G. Zhu, B. Peng, J. Chen, Q. Jing, Z. Lin Wang, Triboelectric nanogenerators as a new energy technology: From fundamentals, devices, to applications, *Nano Energy* 14 (2015) 126–138, <https://doi.org/10.1016/j.nanoen.2014.11.050>.
- [58] Roscoe, *Harvesting Energy from Magnetic Fields to Power Condition Monitoring Sensors* \_preprint version.doc.



**Martha Gerhardt** is a Ph.D. student in the group Functional Nanomaterials at the Kiel University in Germany and part of the collaborative research centre about magnetolectric sensing (CRC1261). She received her master's degree in Material Science in 2020. Her current interests are magnetic field sensing and piezotronics.



**Lukas Zimoch** received the B. Sc. degree in materials science and engineering in 2017 and the M. Sc. degree in materials science and engineering in 2019 from the Christian-Albrechts-University of Kiel, Germany. Since 2020, he is a Ph.D. candidate at the faculty of engineering (Kiel, Germany) and is currently working with magnetostrictive polymer composites in the field of magnetolectric and pressure sensors. Other research interests include tunable inductors, gas sensors for H<sub>2</sub> and volatile organic compounds, as well as superparamagnetic aero-magnets.



**Christian Dorn** received his B.Sc. and M.Sc. degrees in mechanical engineering from Karlsruhe Institute of Technology (KIT) in 2016 and 2018, respectively. He is currently a Ph.D. student in the Computational Materials Science group at the Institute for Materials Science at Kiel University. His research focuses on material modeling and numerical simulations of magnetic materials.



**Eric Elzenheimer** is a postdoctoral researcher at Kiel University, Germany, where he received his Dr.-Ing. in 2022. Since 2015, he has been a member of the Digital Signal Processing and System Theory Group as well as a collaborative research group (CRC 1261) focusing on magnetolectric sensors. His primary research focuses on the functional characterization of magnetic and magnetolectric (ME) sensors, including signal readout and digital signal enhancement for biomagnetometry. Moreover, he is actively involved in preliminary experiments utilizing ME sensor concepts, often in collaboration with Germany's technical authority for metrology and measurement technology, the Physikalisch-Technische Bundesanstalt in Berlin (PTB).



**Christin Bald** received the M.Sc. degree in electrical engineering and business administration from Kiel University, Germany, in 2017, where she is currently pursuing the Ph.D. degree in the Digital Signal Processing and System Theory group embedded in a collaborative research centre for magnetolectric sensors. Her main research interests include magnetic sensor systems and real-time digital signal processing.



**Tjorben Lerg** is a research assistant in the chair of “Digital Signal Processing and System Theory” at Kiel University, where works on the characterization and analysis of magnetic field sensors. He received his Bachelor’s degree in 2022.



**Gerhard Schmidt** received the Dipl.-Ing. degree in 1996 and the Dr.-Ing. degree in 2001, both from Darmstadt, University of Technology, Germany. After his Ph.D., he worked in the research groups of the acoustic signal processing departments at Harman/Becker Automotive Systems and at SVOX, both in Ulm, Germany. Parallel to his time at SVOX he was a part-time professor at Darmstadt, University of Technology. Since 2010 he has been a full professor at Kiel University, Germany. His main research interests include adaptive methods for audio, SONAR, and medical signal processing.



**Johannes Hoffmann** is a doctoral researcher in the Department of Electrical and Information Engineering at Kiel University, Kiel, Germany, where he received his master’s degree in 2020. His research focuses on the application of magnetic and especially magnetoelectric sensors in human movement analysis.



**Stephan Wulfinghoff** received the Dipl.-Ing. degree in 2008 from Karlsruhe University (KIT) in Germany, where he also finalized his Ph.D. thesis in 2014. Subsequently, he worked as engineer in chief at the Institute for Applied Mechanics, RWTH Aachen, Germany until his call for the professorship for Computational Materials Science in Kiel, Germany, in 2018. His main research interests include multiphysics modeling and simulation and multiscale approaches.



**Sören Kaps** is a senior researcher at the Christian Albrechts University Kiel (CAU), Germany, in the chair for “Functional Nanomaterials.” He completed his Ph.D. at CAU in 2015. His primary research revolves around porous materials and the application of additive manufacturing techniques. His work primarily aims to develop innovative designs for memristive devices and magnetic field sensors. Additionally, he has a keen interest in surface interface-related materials science and actively explores advancements in this field.



**Rainer Adelung** is full professor and chairholder of the Functional Nanomaterials group established in 2007 at the Institute for Materials Science, Kiel University, Germany. He received his Ph.D. (rer. nat.) in physics in 2000 from the Institute of Experimental and Applied Physics, Kiel University, and during 2001–2002 he was at Case Western Reserve University in Cleveland (USA) as Feodor Lynen (Alexander von Humboldt) research fellow. In 2006 he finished his Habilitation at the Institute for Materials Science in Kiel and then continued as Heisenberg Professor (DFG grant) starting his own Functional Nanomaterials group in 2007. More information at <https://www.tf.uni-kiel.de/matwis/fnano/de>.



**Michael Höft** is full professor since 2013 at the Kiel University, Kiel, Germany, in the Faculty of Engineering, where he is the Head of the Chair of Microwave Engineering. He received the Dr.-Ing. degree from the Hamburg University of Technology, Hamburg, Germany, in 2002. From 2002–2013, he joined the Communications Laboratory, European Technology Center, Panasonic Industrial Devices Europe GmbH, Lüneburg, Germany. His research interests include active and passive microwave components, (sub-)millimeter-wave quasi-optical techniques and circuitry, microwave and field measurement techniques, microwave filters, microwave sensors, and magnetic field sensors as well as related applications.